



HAL
open science

Prediction of Time Diversity Gain for Earth-to-Satellite Microwave Link Design Based on Real Time Rain Intensity Measurement

Md. Moktarul Alam, Md. Rafiqul Islam, Mohsen Koohestani, Elfatih Elsheikh

► **To cite this version:**

Md. Moktarul Alam, Md. Rafiqul Islam, Mohsen Koohestani, Elfatih Elsheikh. Prediction of Time Diversity Gain for Earth-to-Satellite Microwave Link Design Based on Real Time Rain Intensity Measurement. IEEE Access, 2023, 11, pp.53588-53597. 10.1109/ACCESS.2023.3249962 . hal-04123016

HAL Id: hal-04123016

<https://hal.science/hal-04123016>

Submitted on 2 Oct 2023

HAL is a multi-disciplinary open access archive for the deposit and dissemination of scientific research documents, whether they are published or not. The documents may come from teaching and research institutions in France or abroad, or from public or private research centers.

L'archive ouverte pluridisciplinaire **HAL**, est destinée au dépôt et à la diffusion de documents scientifiques de niveau recherche, publiés ou non, émanant des établissements d'enseignement et de recherche français ou étrangers, des laboratoires publics ou privés.

Received 30 January 2023, accepted 22 February 2023, date of publication 28 February 2023, date of current version 6 June 2023.

Digital Object Identifier 10.1109/ACCESS.2023.3249962

RESEARCH ARTICLE

Prediction of Time Diversity Gain for Earth-to-Satellite Microwave Link Design Based on Real Time Rain Intensity Measurement

MD. MOKTARUL ALAM^{1,2,3}, (Member, IEEE),
MD. RAFIQU L ISLAM¹, (Senior Member, IEEE),
MOHSEN KOOHESTANI^{3,4}, (Senior Member, IEEE),
AND ELFATIH A. A. ELSHEIKH⁵, (Member, IEEE)

¹Department of Electrical and Computer Engineering, Kulliyah of Engineering, International Islamic University Malaysia (IIUM), Kuala Lumpur 53100, Malaysia

²Institut National des Sciences Appliquées, University of Rennes 1, 35708 Rennes, France

³Department of Electrical and Electronic Engineering, ESEO School of Engineering, 49100 Angers, France

⁴Institute of Electronics and Telecommunications of Rennes (IETR), University of Rennes 1, 35042 Rennes, France

⁵Department of Electrical Engineering, College of Engineering, King Khalid University, Abha 62529, Saudi Arabia

Corresponding author: Md. Moktarul Alam (moktarulee@gmail.com)

This work was supported by the Deanship of Scientific Research at King Khalid University through the Research Group Program under Grant R.G.P.1/180/43.

ABSTRACT The propagation impairments by rain strongly affect the earth-to-satellite links operating at frequencies higher than 18 GHz mainly due to the severe performance degradation of satellite communication system. The time diversity technique with appropriate time delay between successive transmissions has been found effective in mitigating the rain fade. However, time diversity analysis demands measured rain attenuation data, where the latter is unavailable at most of the places to be able to design future high frequency links. The time diversity gain prediction model has been found to be robust for time diversity improvement. Here, we propose a new model for the rain rate with and without the time delay considering the three variables of rain rate, time delay and frequency. The rain rate and time delay functions were first used to derive the constants by the regression from the rain rate and rain rate gain. The constant for the frequency function was then extracted from the cumulative distribution function of the attenuation predicted by the analytically obtained ITU-R and gain equations. The proposed model was validated using one-year rain rate and attenuation data measured at two different locations in Malaysia demonstrating a 7% prediction inaccuracy when compared to the existing models, therefore, it can be reliably used for future earth-to-satellite link designs by using measured rain rate at any higher frequencies.

INDEX TERMS Rain rate, rain attenuation, time delay, time diversity technique.

I. INTRODUCTION

Charged particles in the ionosphere, rain, ice, fog, clouds, and moist air in the troposphere are the main parameters affecting the propagation of electromagnetic (EM) waves through the atmosphere. Rain is known to have the most significant impact on the troposphere [1]. The troposphere scatter propagation interferes with ground transmission and

The associate editor coordinating the review of this manuscript and approving it for publication was Lei Zhao¹.

receiver functioning in the same frequency band [2]. The dispersed signal noise might have a direct impact on the system's performance. The preliminary signal absorption lost in a wide range of frequencies above 10 GHz is called rain fade, which depends on the climate, path attenuation, and primarily rain attenuation [3]. The most desirable spectrum to satisfy the broadband needs is the frequency range between 1 and 10 GHz. Rain initiated depolarization is resulted from differential attenuation and phase shift due to non-spherical raindrops. As the size of rain drops increases, their shape tend

to transform from spherical (the preferred shape because of surface tension forces) to oblate spheroids with an increasingly pronounced flat or concave base produced from aerodynamic forces acting upward on the drops [4]. Moreover, raindrops may also be horizontally inclined due to the vertical wind gradients [5]. The depolarization characteristics of a linearly polarized radiowave depend significantly on the transmitted polarization angle. The determination of the rain depolarization characteristics requires the knowledge of the canting angle of the raindrops, defined as the angle between the major axis of the drop and the local horizontal [6].

The system performance, architectural factors, and operating frequency ranges must all be considered when using the fade mitigation methods (FMT). In terms of cost and advantages, time diversity has been found to be a viable approach for delaying time that may enhance the rain fade among FMTs in an Earth-to-satellite connection that is experiencing severe channel fading [7]. Measured rain attenuation time series with and without time delay are often used to assess the performance of time diversity. It estimates the likelihood of rain attenuation excess with and without delay. The increase in time variety is a sign of progress. In Malaysia, an empirical model was developed to forecast the time diversity gain function based on observed data to assess the chance of rain attenuation excess [8]. The gain of time diversity relies on the yearly parameter, measured in decibels (dB) with the cumulative rain attenuation of the distributions (known as transmission time delay) [9], utilized for execution of the assessment and mitigating technique [10]. Time delay slots are affected by weather conditions.

There is in fact limited research on the performance of time variation. In [11], it has been demonstrated that rain attenuation via earth-to-satellite link is closely proportional to rain intensity, which attenuation variation occurs throughout the propagation route as a result of rain variation. Previously synthetic storm technique (SST) technique was used [12], [13], [14] to predict rain attenuation time series from measured rain rate time series with and without time delays. However, when compared to measured gain, the technique consistently tends to overestimate gain. The predicted rain attenuation with time delays are used to calculate time diversity gain at any desired frequency for the SST observation in the tropical area (Malaysia). All related studies have used measured rain attenuation data with a time delay to investigate time diversity gain and provided improvement [15]. However, most of this data are unavailable, particularly in the Ka and V-bands, which must be constructed for future highly dependable communication systems [16], [17], [18].

This paper proposed time diversity gain modeling by using measured rain rate. In this model, all the variables are considered, including the measured rain rate, time delay, and frequency. Firstly, $G_1(R\%,p,T)$ is expressed as rain rate gain and calculated based on measured rainfall rate with and without time delay. Furthermore, utilizing ITU-R P.618-13, $G_2(f)$ is

defined based on the cumulative distribution function (CDF) of rain attenuation, and the attenuation gain is determined using the time delay technique 1 to 60 minutes. At various frequencies, the constant is determined for both attenuation and attenuation gain combinations. These two functions are combining to predict the attenuation gain model.

Section II explains the technique of time-diversity by using SST method and compare the predicted result with measurement. Section III describes the bucket gauge of rain rate and explain briefly data collection and data integration. The measured rain rate with time delay method is proposed in Section IV. Section V is shown the result of the modeling and compare the gain with measured in Section VI. Section VII describes the overall significance of modeling.

II. TIME DIVERSITY TECHNIQUE BY USING SST

This section provides a technical overview of the various rain rate integration with time series and SST. In addition, a study of the present state of practice in authentication is performed to examine the current research trend.

The SST approach is used to estimate the probability of long-term rain rate using a series of measurements made during rain attenuation, as well as daily and service-based information [16]. The SST technique is used to develop communication satellite systems, and in the future, its performance can be assessed to predict the attenuation by using rain rate time series. Equations (1-4) describe the SST technique mathematically.

$$A(X) = K_A \int_0^{L_A} R^{\alpha_A} (X_0 + \Delta X_0, \xi) d\xi + K_B R^{\alpha_B} \int_{L_B}^{L_A} R^{\alpha_B} (X_0, \xi) d\xi \quad (1)$$

where $A(x)$ = The attenuation measured at a particular distance, K_A = coefficient at water temperature of 20°C, R = the measured rain rate time series definition, α_a = coefficient for drop size distribution at 20°C, ξ = The distance of the satellite path, K_B = coefficient at water temperature of 0°C and α_a = coefficient for drop size distribution at 0°C. It is initiated by a certain attenuation in the case of satellite paths [17]. The Inverse Fourier transform on spatial variation of attenuation $A(x)$ in Equation (1) is applied and the time variation of attenuation $A(t)$ is derived in Equation (2).

$$A(t) = K_A R^{\alpha_A}(t) L_A + r^{\alpha_A} K_B R^{\alpha_B}(t) (L_A - L_B) \quad (2)$$

where $A(t)$ = the rain attenuation at time t , $R(t)$ = the rain rate time series, L_A = Rain layers at a temperature of 20 °C, L_B = melting layers at a temperature of 0 °C.

$$\Delta x_0 = \Delta L \cos(\theta) = h / \tan(\theta) \\ \Delta L = L_N - L_* = h / \sin(\theta) \quad (3)$$

As a consequence of the time series relating to the rate of rain, an attenuation data set is obtained in Equation (3). During the rain, v = the observed wind velocity, and θ = the

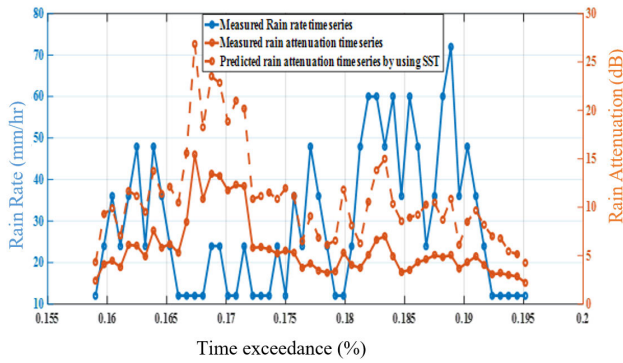


FIGURE 1. An example of an event where measured rain rate and measured attenuation are compared with converted attenuation using SST.

elevation angle. Equation (4) calculates the attenuation from a probability rain rate distribution using the rate time series.

$$A = [C_0 K_{AR}^{\alpha A} + (1 - C_0) K_B 3.1416 R^{\alpha B}] L^m \quad (4)$$

The latitude dependent C and L constants are given by the average longitudinal diagonal route of precipitation [19]. In equations, the parameter m is utilized to take values. The general constants for the SST [20] model of precipitation rate is K and α . This enables for the measurement of rain attenuation (dB/km) using two layers of precipitation, A and B.

The measured rain rate and attenuation data 2009 were observed and compared with SST predict rain attenuation. For validation, the data collected by receiving beacon measurement of the signal was situated at University Sains Malaysia (USM) (4.39° N, 100.98° E) at a height of 57 m above mean sea level. The signal was received at a frequency of 12.255 GHz and an elevation angle of 40.10° from the SUPERBIRD-C satellite. The low-noise block (LNB) was coupled with the antenna to convert the ku-band to an intermediate frequency, and the antenna dish was 2.4 m in diameter.

The SST equation (1-4) was used to predict rain attenuation using the 2009 measured rainfall rate time record. Fig. 1 summarizes and depicts the parameters of the rain rate time series with expected and observed attenuation.

Fig. 1 shows that calculated SST attenuation and rain rate time series have similar features. In earlier analysis, SST technique [28], [29] was implemented with different velocities from 1 to 20 m/s where it was found that the predicted rain attenuation characteristics match well with that of the measured rain rate at storm velocity of 11 m/s. The most important finding is that utilizing SST as a function of observed rainfall rate, attenuation rises quickly. This seems to be reasonable since most tropical rainfall is of short duration and high intensity.

SST simulation in non-real time is achievable between 12 GHz and 100 GHz. Matricciani developed the SST model [18], which takes frequency and time into consideration. He used the SST model to transform real-time rain

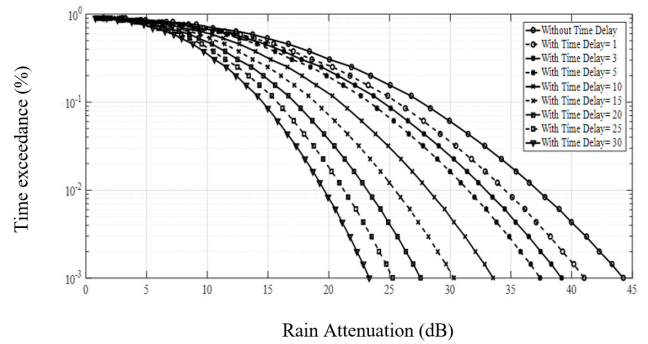


FIGURE 2. Cumulative distributions function of predicted rain attenuation with time delays by using SST.

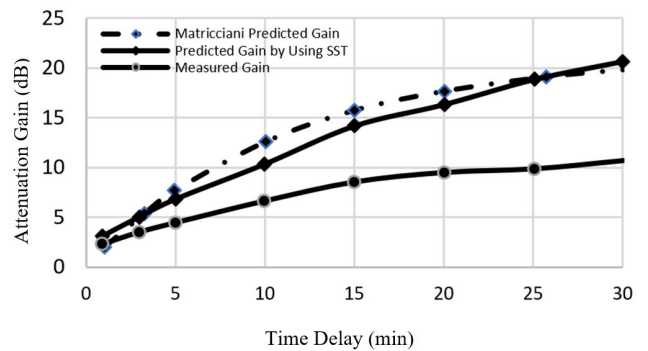


FIGURE 3. Comparison among measured rain attenuation gain, predicted rain attenuation gain by using SST, predicted rain attenuation gain by using SST and Matricciani model gain [12] at 0.01% for 12 GHz.

rate data to rain attenuation time series. It has been converted to rain attenuation using equation (4) and a complementary cumulative distribution function has been developed by attenuation time series to utilize the Matricciani concept [18]. After utilizing SST with varied time delays to transform the delaying rain attenuation time series. Fig. 2 shows the complementary cumulative function with and without time delay using the conversation delaying time series.

Rain attenuation is measured using a time delay of 1 to 30 minutes, and it is found that without the time delay, the amount of attenuation was 36 dB for 0.01%, but after the 30 minute delay, the amount of attenuation is 19 dB. As a consequence, the time delay approach may be used to mitigate attenuation.

The predicted gain of one year was estimated using the general formula of attenuation gain $GA_{Td}(\%p) = A(\%p) - A_{Td}(\%p)$ by applying the SST technique and delaying various periods. Fig. 3 shows a comparison of the expected gain with the observed gain and Matricciani's predicted gain [12] for the same time period.

The G_A predicted by SST is compared to the gain observed, and the measured G_A is shown to be underestimate than the gain predicted by SST. After a delay of 1 to 30 minutes, the difference between them is 10 dB, which is detected after 30 minutes. Thus, 51% of these errors are observed.

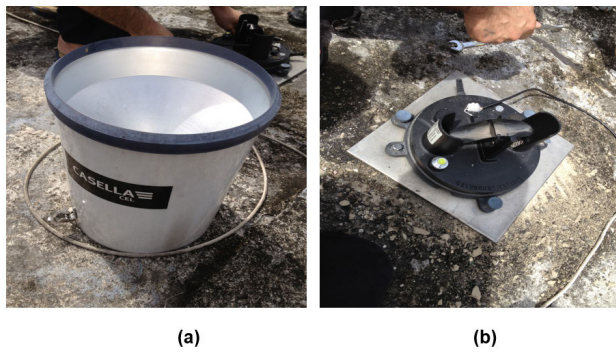


FIGURE 4. (a) Casella rain gauge of Tipping Bucket type and (b) mechanism of Tipping Bucket.

SST estimated G_A has been compared to Matricciani predicted G_A [12] and found to be fairly similar. There is a 2 dB difference and a 13% inaccuracy between the two measurements, even with a 10 minute delay.

The benefits indicated by the SST and Matricciani models [12] are far from being measured. As a consequence, a higher-frequency SST model will be built. The SST predicted gain is found to be much higher when compared to the measured attenuation gain at the same frequency as shown in Fig. 3 [12]. In this paper, the predicted rain attenuation with and without delays are proposed by using measured rain rate distributions with and without delays by applying the ITU-R prediction method as illustrated in section IV.

III. MEASUREMENT AND DATA COLLECTION

A rain gauge was put up at the International Islamic University in Malaysia to monitor the rain rate during a propagation experiment campaign. A real-time rain gauge at IIUM was used to record rainfall data for a year beginning on January 1, 2014, to December 31, 2014. The data logger was integrated with buckets in the same casing and recorded rain rate with 10-seconds integration time. The data was missing because of battery goes down. Those hours are extracted and used to calculate the availability and presented in Table 3. Rain gauge bucket size and tripping bucket mechanism are depicted in Fig. 4(a) and 4(b). In order to collect rain, the bucket has a fixed amount of water on one side of it. When one side of the bucket is full of discharged water, the other side of the bucket will switch to a filling position. 0.2 mm of water will be collected in each bucket. The Casella tipping bucket type of rain gauge has two equal size buckets with 0.2 mm rain water accumulated from the rain gauge drum. The data logger is integrated together with rain gauge which records the number of tips per 10-second in terms of rain height in mm. As a result, data will be captured as soon as the bucket is modified. There is a detailed description of the rain gauge and a sample of gathered data in Table 1 and Table 2. Data was collected by using tripping buckets with a 10-second integration time and during a minute-long integration, the six data are combined together. The recorded 1-minute rain rate

TABLE 1. Specification of real-time rain gauge.

RG's Geographic Range	101.732° E
RG's latitude	3.257° N
Size of a Bucket	0.2 mm
Magnification	200 cm ²
Approximation	±1% at 26mm/hr
Transducer	Magnet/Reed switch
Temperature range for operation	1°C to 85°C
Amount produced	Contact closure
Weight	3.2 kg
The current rating at its maximum	500 mA
Archiving of data	64K
Time for integration	10 second

TABLE 2. A sample of data collected on 29 April, 2014.

Date	Time	Volts	mm
29/4/2014	16:33:05	11.55	0.2
29/4/2014	16:33:15	11.54	0
29/4/2014	16:33:25	11.54	0
29/4/2014	16:33:35	11.54	0.2
29/4/2014	16:33:45	11.54	0.2
29/4/2014	16:33:55	11.55	0
29/4/2014	16:34:05	11.54	0.2
29/4/2014	16:34:15	11.54	0
29/4/2014	16:34:25	11.54	0.2
29/4/2014	16:34:35	11.54	0.2
29/4/2014	16:34:45	11.54	0.2
29/4/2014	16:34:55	11.54	0.2
29/4/2014	16:35:05	11.54	0.2
29/4/2014	16:35:15	11.54	0
29/4/2014	16:35:25	11.54	0.2
29/4/2014	16:35:35	11.54	0.2
29/4/2014	16:35:45	11.54	0
29/4/2014	16:35:55	11.54	0.2
29/4/2014	16:36:05	11.54	0
29/4/2014	16:36:15	11.54	0.2
29/4/2014	16:36:25	11.54	0
29/4/2014	16:36:35	11.54	0.2
29/4/2014	16:36:45	11.54	0
29/4/2014	16:36:55	11.54	0.2

data is used to construct the monthly and annual cumulative distributions. An approaching idea of rain rate with and without a time delay (1, 3, 5, 10, 20 and 30 minutes) is used to observe the monthly and yearly rain rate distribution by using equations (5) and (6). Modeling of time diversity gain is done by using measured data from January to December of 2014.

One minute integration time is needed to analyze data captured in 10 second integration time intervals. A conversion from mm/10 second to mm/hr is required [29]. As a result, the integration times were represented graphically using the

TABLE 3. The availability of measured rain data at 2014.

Month	Data missing	Availability
January	27.66	96.28%
February	0.71	99.89%
March	15.33	97.94%
April	6.55	99.09%
May	5.30	99.29%
June	24.97	96.53%
July	6.30	99.15%
August	12.00	98.39%
September	78.45	89.10%
October	5.91	99.21%
November	0.01	100.00%
December	3.54	99.52%

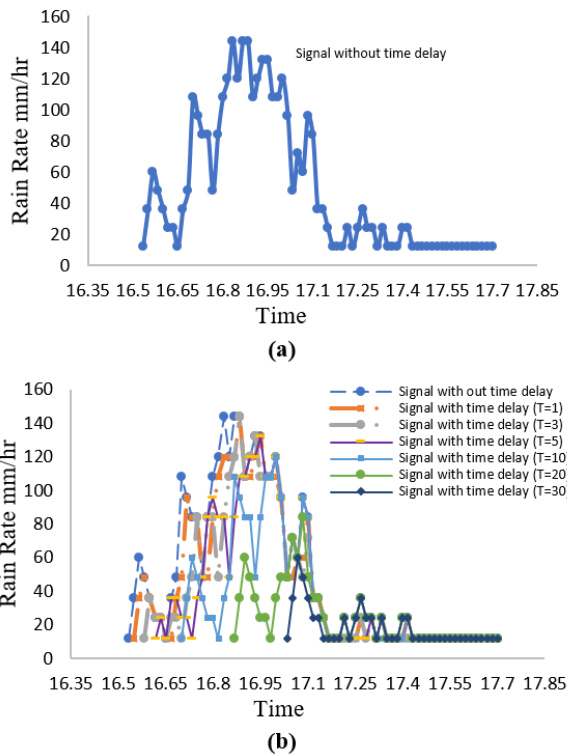


FIGURE 5. (a) An event of real time rain rate variation and (b) time delay method applied for improvement by using measured rain rate in April 29, 2014.

equations (5-6) are shown below:

$$r_{\tau} = \sum_{k=t_{st}}^{t_{end}} r_k \tag{5}$$

where, r_k = rainfall volume at time k, mm r_{τ} = rain volume accumulation for 10s, 30s and 1-minute t_{st} = time to begin t_{end} = the end of time

The rain rate, R (mm/hr) is obtained from the following equation

$$R = r_{\tau} * T_{\tau} \tag{6}$$

where, $T_{\tau}=60$, for $\tau=1$ min Equations (5) and (6), measured one year data are converted to 1-minute integration time and analyzed for statistical distributions with and without time delay.

IV. PROPOSED TIME DIVERSITY TECHNIQUE BY USING RAIN RATE

Many researchers are able to mitigate rainfall degradation by using the time variation technique to investigate the concept of signals received with proper delays. Real-time rainfall changes and the time delay are displayed in Fig. 5(a) and Fig. 5(b).

It is shown in Fig. 5(a) that the greatest rate of rainfall observed is 146.0 millimeters per hour (mm/h). While its significance reduces with the delay, The greatest values of rainfall obtained after 1, 3, 5, 10, 20, and 30 minutes of delay are 134, 122, 110, 95, 82, and 58 mm/hr, respectively.

The rain rate equation is derived from the principle of rain attenuation equation (7) and real-time rainfall is presented using the CDF equation (8) of performance rainfall rate.

$$\Pr(R) = \Pr[R(t) > R] = \int_0^{\infty} \xi[R(t)]dR \tag{7}$$

In addition to real time and time delay, rainfall rate is given as a joint probability function of equation (8).

$$\begin{aligned} &\Pr [R(t) > R, R(t + T_d) > R] \\ &= \int_R^{\infty} \int_R^{\infty} \gamma [R(t), R(t + T_d)] dR(t)dR(t + T_d) \end{aligned} \tag{8}$$

$R(t+T_d)$ is used to express real-time rainfall rate with time delay, and $[R(t), R(t+T_d)]$ is used to express the combined probability of time delay with rainfall rate. Combining equations (7) and (8), the minimal rain rate with a time delay is represented in equation (9).

Equation (9) gives the time statically gain, which is the basis for the time diversity rain rate gain. Any percentage of a time delay may be used to increase the rain rate gain, as shown in the calculation (10)

$$R_{TD} = \min[R(T), R(t + T_d)] \tag{9}$$

$$GR_{TD} = R(T_d) - R_{TD} \frac{mm}{hr}$$

$$GR_{TD}(\%p) = R_{\%p} - R(T_d)\%p \tag{10}$$

Rain rate $R_{\%P}$ and a joint distribution $R_c(T_d)\%P$ connected to time delay T_d may be used to establish the long term yearly distribution with equal probability for statistical benefit from time diversity.

V. MODELLING OF TIME DIVERSITY GAIN

Although attenuation occurs as a result of rain, the model was developed using the observed rain rate. As a result, rain rate was used rather than attenuation since the former is widely available. Based on Malaysia's observed rainfall rate, a time diversity gain (G_A) model has been presented. The rain, time delay, and frequency are all the factors considered in this model. The constants are first obtained by the regression from the increase in rainfall rate. Second, the gain is calculated using the CDF and the attenuation data predicted by the constant ITU-R P.618-13 as a function of the frequency. The suggested attenuation gain model is formed by multiplying these two functions together.

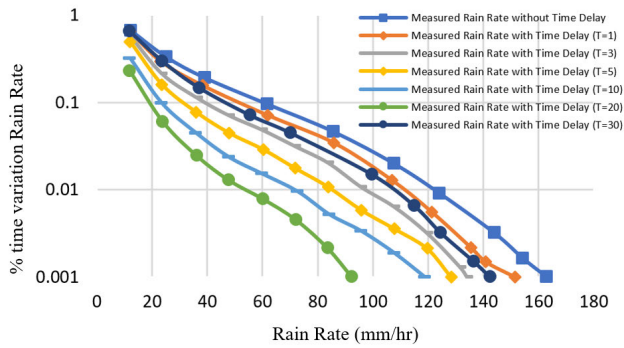


FIGURE 6. Complementary cumulative distributions of measured one-year rain rate without and with several time delays.

TABLE 4. Rain rate with and without time delay.

Time (minute)	Rain Rate (mm/hr)
0	125
1	114
3	108
5	96
10	85
15	78
20	74
25	66
30	56

The increase in time diversity is determined by two factors: first, the observed rain rate, $R_{\%P}$ (mm/hr) with a time delay T (minute); and second, the frequency f (GHz). As a result, the following function may be presented to establish an attenuation gain model based on the time diversity gain provided by equation (11):

$$G_A = G_1(R_{\%P}, T)G_2(f) \quad (11)$$

A. MODELLING OF $G_1(R_{\%P}, T)$

The 2014 rain rate data with various time delays was used to develop a CDF for this modeling. Fig. 6 presents the annual rainfall rates, which were derived using statistical equations (7-9).

Fig. 6 and Table 4 show the recorded rain rate distribution with and without period variation. For time delays of 1, 3, 5, 10, 20, 25 and 30 minutes, the rain rate is 125 mm/hr without time variety, whereas it is 114, 108, 96, 85, 78, 74, 66 and 56 mm/hr with time variation, respectively. T, the effective rain rate may be lowered to 10, 15, 25, 29, 39, 50, and 68.5 mm/hr with the same time delays, respectively.

Fig. 7 plots the GR_{TD} estimates from equations (8-10) versus $R_{\%P}$. The gain G_1 increases linearly with delay time T. As a result, a conversion strategy to predict rain rate with delay $R_{p\%P}$ (mm/hr) from measured $R_{m\%P}$ (mm/hr) without delay has been proposed. The Hodge’s site diversity formula (12) was used to calculate the diversity gain G [20].

$$G = G_0(1 - e^{-BT}) \quad (12)$$

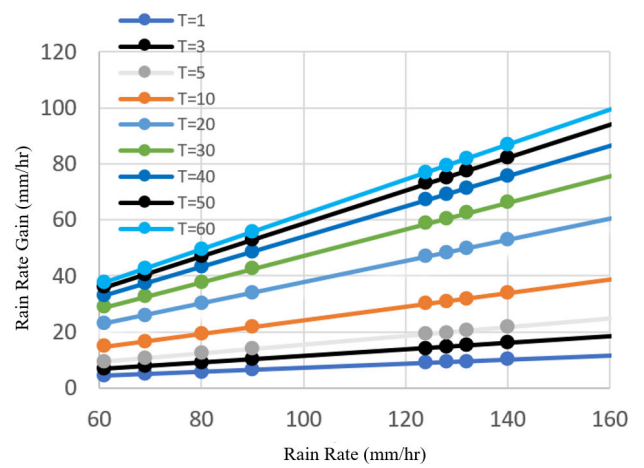


FIGURE 7. Measured rain rate gain $GR_T D$ (mm/hr) versus measured rain rate $R_{(m\%P)}$ (mm/hr) a function of time delays.

G_0 is a function of single site attenuation gain, where T is represented in time delay and B is the coefficient with time delay T. The rain rate gain is calculated using the Hodge Site diversity concept based on a given quantity of recorded rain rate and time delay [21]. $G_1(R_{\%P}, TD)$ modeling is also stated as $R_{\%P} =$ Predicted rain rate and TD is time delay expressed as T.

$$G_1(R_{\%P}, TD) = R_{m\%P}(1 - m(T)) \quad (13)$$

The Hodge equation (15) G denotes $R_{p\%P} =$ Predicted Rain Rate, G_0 denotes $R_{m\%P} =$ measured rain rate and e^{BT} denotes $m(T) =$ the smooth function of time delay. Equation (16) determines the Hodge concept, which is represented as equation (14)

$$\begin{aligned} R_{p\%P} &= R_{m\%P}(1 - m(T)) \\ m(T) &= (ae^{-bT} + c) \end{aligned} \quad (14)$$

Fig. 6 and Fig. 7 are required for equation (14). Those figures are used to determine the coefficients a, b, and c. They are used to plot $m(t)$, which is presented in Fig. 8 with a time delay T. Fig. 5 shows a satisfactory match with $m(t)$ through coefficients a, b, and c when utilizing a linear and broad model of exponential combination. Regression coefficients is 95% confidence bounds.

The rain rate gain at time delay T is denoted by GR_{TDn} while the same time delay rain rate gain is defined by $R_{TD(n-1)}$. Both parameters are determined by the number of rain rate gains and are denoted by n. The mean value is calculated using equation (15).

$$a = \text{mean} \sqrt{\left(\frac{GR_{TDn} - GR_{TD(n-1)}}{GR_{TDn}} \right)} \quad (15)$$

The yearly time variation excess is defined by the percent p, and R_{mTDn} is determined by the time delay confidence level and computed using R_m . Using the formula (16), get

the mean value of b.

$$b = \text{mean} \left(\%p * \sum_{n=1}^n R_{mTD_n} - R_{mTD_{n-1}} \right) \quad (16)$$

The observed rain rate at any percentage is computed using R_m to determine $R_m\%p$. Using the formula (17), get the average value of c.

$$C = \text{mean} \sum_{n=1} (GR_{TD_n} - GR_{TD_{n-1}}) / R_{m\%p} \quad (17)$$

The values of $a=0.65$, $b=0.035$, and $c = 0.30$ were calculated using equations (15-17). The constant value is provided in equation (18) to derive the function $m(T)$.

$$m(T) = (0.65e^{-0.035T} + 0.30) \quad (18)$$

The model of $G_1(R\%p, T)$ is calculated by combining equations (15-18), which resulted in the final expression of the predicted rain rate equation (19).

$$G_1(R\%p, T) = R_{m\%p}(0.65e^{-0.035T} + 0.30) \quad (19)$$

B. MODELLING OF $G_2(f)$

Rain attenuation predictions could be used to calculate $G_2(f)$ as a function of frequency. Using time delay of 1 to 30 minutes, the ITU-R P.618-13 prediction technique [21], [22], [23], [24] is utilized to estimate the rain attenuation on the earth-to-satellite link using the recorded rain rate. Probability rain attenuation has been determined at various percentages using equations (20) and (21). Equation (22) of ITU-R 837-7, as well as equations (2) and (23) of ITU-R 618-13, were applied. A rain rate of 0.01% has been obtained from the table based on the time delay. The equation (20) was used to calculate the time delay rain attenuation, that was represented in Fig. 8. The expected gain was calculated using various frequencies using the general gain equation, as illustrated in Fig. 9.

$$\begin{aligned} \gamma_A &= k_H R^{\alpha_H} \\ A_{0.01} &= \gamma_A * L_{\text{eff}} \\ A_p &= A_{0.01} \left(\frac{p}{0.01} \right)^{-0.655+0.033 \ln(p)-0.045 \ln(A_{0.01})-\beta(1-p) \sin \theta} \end{aligned} \quad (20)$$

The rain attenuation gains are obtained similarly from 10 to 60 GHz with time delays from 1 to 60 minutes and presented in Fig. 8. The rain attenuation increases exponentially with frequency as shown in Fig. 9. The concept of $G_2(f)$ is taken from Matricciani model [19]. The study of $G_2(f)$ in Fig. 10 shows how $G_2(f)$ varies as a function of a constant d for all frequencies in the range from 10 to 60 GHz. Based on [19], Fig. 10 can be modeled by a line as follows:

$$\begin{aligned} G_2(f) &= m(f) \\ m(f) &= \ln(df) \end{aligned} \quad (21)$$

Based on ITU-R equation, d is defined as the effective path length which is calculated from average attenuation gain by using equation (22)

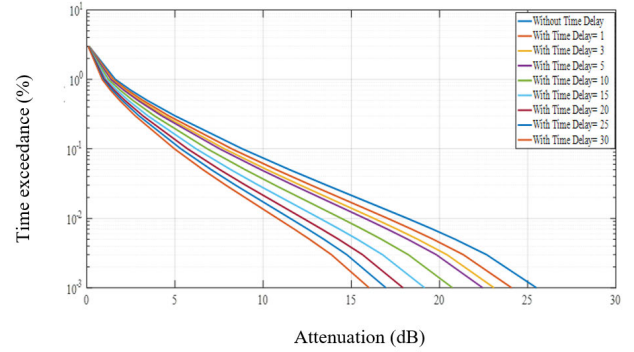


FIGURE 8. Complementary cumulative distribution function of predicted rain attenuation using ITU-R P.618-13 formula and measured $R_{0.01\%}$ with delays.

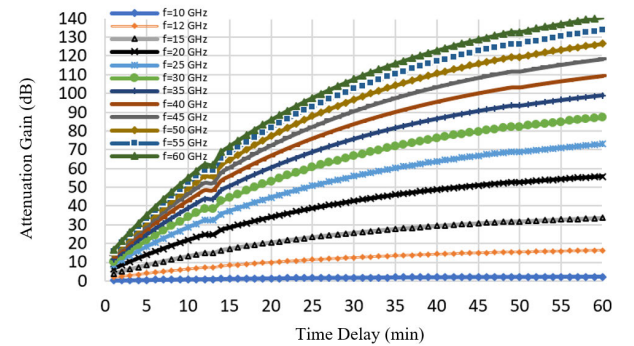


FIGURE 9. Attenuation gain obtained by marginal rain attenuation from 0 to 150 dB, at 10 to 60 GHz as the function of Time delay.

Using Fig. 9, $m(f)$ is plotted with frequency f and displayed in Fig. 10. As observed, the smooth function can be proposed by the following expression as

$$\begin{aligned} m(f) &= \ln(d) \text{ when } d = 0.103 \\ G_2(f) &= \ln(d) + \ln(f) \\ &= \ln(df) \\ &= \ln(0.103 * f) \end{aligned} \quad (22)$$

C. PROPOSED TIME DIVERSITY GAIN MODEL

G_A is defined as attenuation gain, which is a function of measured rain rate, time delay and frequency. The model usually can be used to predict attenuation gain for the place where measured rain attenuation data is not available. Rain attenuation at any percentage of time outage for any desired frequency and time delay can be predicted using equation (23) based on equations (18), (20) and (22). The model requires the measured rain intensity statistics at that location.

$$G_{A\%p} = R_{m\%p}(0.65e^{-0.035T} + 0.30) * \ln(0.103 * f) \quad (23)$$

Here, G_A = Attenuation Gain, dB %P = Time exceedance percentage in logarithm scale R_m = Measured Rain Rate, mm/hr T =Time Delay, min f = Frequency, GHz

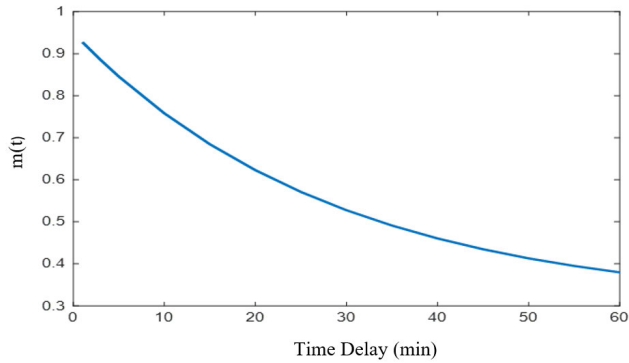


FIGURE 10. Attenuation gain obtained by marginal rain attenuation from 0 to 150 dB, at 10 to 60 GHz as the function of Time delay.

The time diversity gain at any desired frequency may be estimated using the proposed model in equation (23), that is based on the time delay and observed rain rate values for earth-to-satellite links at various exceeding time percentages.

VI. VALIDATION OF THE PROPOSED MODEL

The one-year rain rate and rain attenuation data recorded at two sites in Malaysia are used to confirm the predicted diversity gain by implementing equation (23) for one-year rain rate and rain attenuation data. In Malaysia, rain attenuation data were recorded at 12.225 GHz in USM using the Super Bird C satellite with an elevation angle of 40.10° and at 12 GHz in Kuala Lumpur using the MEASAT-1 satellite with an elevation angle of 77.40° [29], [30], [31]. With time delays of 1, 3, 5, 10, 15, 20, 25, and 30 minutes, the observed time diversity gain for both frequencies is calculated and compared to those predicted by the model. From August 1996 to July 1997, [29] and USM for 2009 [31], the cumulative distribution of recorded real time rain rate is utilized to calculate $R_{\%}P$. Also, time delays of 1, 3, 5, 10, 15, 20, 25, and 30 minutes were utilized to validate the cumulative distribution of recorded rain attenuation at two sites in Malaysia are compared to the equation’s predictions (23). Fig. 11 shows the predicted G_A versus the measured G_A from Kuala Lumpur.

$$RMSE = \sqrt{\frac{\sum_{i=1}^{Td} \|Measured - Predicted\|^2}{Td}} \quad (24)$$

Here Td = Time delay.

The equation (23) is used to determine the attenuation gain after delaying the rain rate by 1 to 30 minutes, and the predicted G_A is compared with the measured G_A . Equation (24) based on statistical estimate [25] are used for comparison and is shown in Fig. 11. According to comparison, 0.01% with 5-minute delay, occurs 0.1 dB and the rest are same up to a 20-minute delay. The slightly variation, 0.01%, occurs at 0.6 dB with a 25 minute delay with a 4% inaccuracy. The largest difference is 0.3 dB with 30 minutes delay with a 5% inaccuracy. As a result, the gain computed using the observed rain rate and equation (23) is statistical to the gain obtained using the one-year attenuation data.

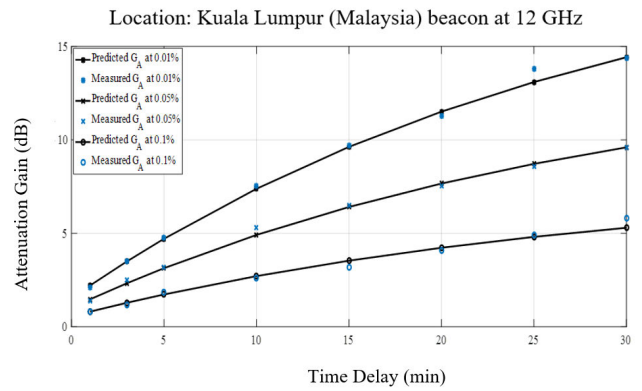


FIGURE 11. Comparison between time diversity gain measured at Kuala Lumpur with that predicted by proposed equation (24).

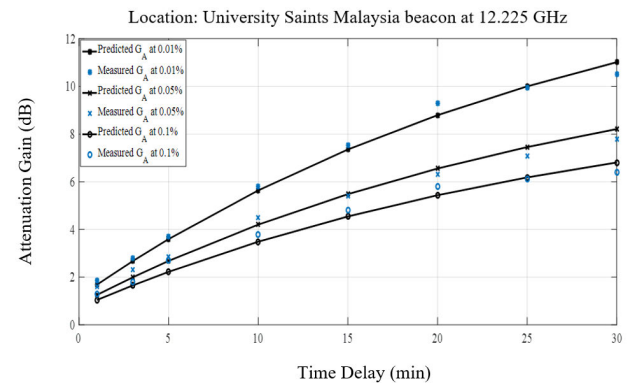


FIGURE 12. Comparison between time diversity gain measured at USM with that predicted by proposed equation (24).

Fig. 12 depicts the comparison between predicted and observed G_A from USM measurements. Up to a time delay of 15 minutes at 0.01%, the gain predicted by the model is remarkably similar to the actual gain. Up to 20 minutes delay, it underestimates and overestimates with 30 minutes delay. In both situations, the difference is 0.6 dB, which equals to 7% inaccuracy. At 0.05%, the greatest difference is 0.4 dB, with a 5% inaccuracy. It underestimates till 20 minutes delay and overestimates at 30 minutes after the delay at 0.1%. The largest discrepancy is 0.4 dB, indicating 6% inaccuracy. As a result, using the measured one year rain data, the predicted G_A based on equation (23) can mitigate the attenuation, hence, instead of measuring G_A data in the future, it can be used to design microwave links.

VII. CONCLUSION

The satellite communication system performance suffers from severe degradation at high frequencies in tropical and equatorial climate. Time diversity is one of the techniques commonly used for mitigation of the rain fade. It is clear, the technique of time diversity is suitable for applications such as data transfer process that not needed until the rain fades

over. However, time diversity analysis requires measured rain attenuation data which are not available at most of the places. This paper evaluates a method to utilize 1-minute rain rate to analyse rain rate gain which is used for time diversity gain at any desired frequency. It is assumed that rain rate gain with delay can represent rain attenuation gain with delay for same period of time at same location. Measured 1-year rain rate distribution with and without delay were used for rain rate gain. Measured rain rate is used to predict rain attenuation distributions by ITU-R method. This distribution with and without delay is found very similar characteristics with those obtained by measurements. Predicted rain attenuation distribution is analysed to estimate attenuation gain and is compared with measured attenuation gain for different frequencies. The predicted attenuation gain is found close to measured one. In proposed model is used also three variables namely rain rate, time delay and frequency. Firstly, rain rate and time delay functions are used together, and constants are derived by regression from rain rate and rain rate gain. Secondly, constant for frequency function is derived from CDF of attenuation predicted by ITU-R and gain obtained analytically. These two functions are combined together and the proposed model of attenuation gain (G_A) is developed. The proposed time diversity gain, G_A is evaluated using one-year rain rate and rain attenuation data from two Malaysian locations. The developed model is compared to the measured time diversity gains at Ku-bands with time delays of 1, 3, 5, 10, 15, 20, 25, and 30 minutes. The gains predicted by the proposed model are almost similar to observed gains at 12.0 and 12.225 GHz for two sites, Kuala Lumpur and Penang, with a maximum difference of 7%. As a result, utilizing recorded rain rate distributions at any higher frequencies, the suggested model will be highly beneficial in the future for earth-to-satellite link design.

REFERENCES

- [1] C. I. Kourogorgas, A. D. Panagopoulos, S. N. Livieratos, and G. E. Chatzarakis, "Time diversity prediction modeling using copula functions for satellite communication systems operating above 10 GHz," in *Proc. 31st Gen. Assem. Sci. Symp. (URSI GASS)*, Aug. 2014, pp. 10–14.
- [2] S. Shrestha and D.-Y. Choi, "Diurnal and monthly variations of rain rate and rain attenuation on Ka-band satellite communication in South Korea," *Prog. Electromagn. Res. B*, vol. 80, pp. 151–171, 2018.
- [3] A. F. Ismail, J. Din, A. R. Tharek, M. R. Islam, and K. Abdullah, "Analyses of rain fade countermeasure technique time diversity at 26 GHz," in *Proc. IEEE Asia-Pacific Conf. Antennas Propag.*, Aug. 2012, pp. 217–218.
- [4] P.-D.-M. Arapoglou, A. D. Panagopoulos, and P. G. Cottis, "An analytical prediction model of time diversity performance for Earth-space fade mitigation," *Int. J. Antennas Propag.*, vol. 2008, pp. 1–5, Jan. 2008, doi: 10.1155/2008/142497.
- [5] C. I. Kourogorgas, S. N. Livieratos, A. D. Panagopoulos, and G. E. Chatzarakis, "Modeling of joint rainfall rate and rain attenuation statistics using Archimedean copula functions," in *Proc. 8th Eur. Conf. Antennas Propag. (EuCAP)*, Apr. 2014, pp. 509–512.
- [6] Q. W. Pan, J. E. Allnutt, and C. Tsui, "Evaluation of diversity and power control techniques for satellite communication systems in tropical and equatorial rain climates," *IEEE Trans. Antennas Propag.*, vol. 56, no. 10, pp. 3293–3301, Oct. 2008, doi: 10.1109/TAP.2008.929448.
- [7] L. J. Ippolito, "Radio propagation for space communications systems," *Proc. IEEE*, vol. 69, no. 6, pp. 697–727, Jun. 1981, doi: 10.1109/PROC.1981.12049.
- [8] K. M. Udofia and I. E. Otung, "Evaluating time diversity performance on an on-board processing satellite to Earth station downlink," in *Proc. 2nd Int. Conf. Next Gener. Mobile Appl., Services, Technol.*, Sep. 2008, pp. 325–330.
- [9] S. K. Kotamraju and C. S. K. Korada, "Precipitation and other propagation impairments effects at microwave and millimeter wave bands: A mini survey," *Acta Geophys.*, vol. 67, no. 2, pp. 703–719, Apr. 2019.
- [10] S. Ventouras, S. A. Callaghan, and C. L. Wrench, "Long-term statistics of tropospheric attenuation from the Ka/U band ITALSAT satellite experiment in the United Kingdom," *Radio Sci.*, vol. 41, no. 2, pp. 1–19, Apr. 2006, doi: 10.1029/2005RS003252.
- [11] D. Pimienta-Del-Valle, J. M. Riera, and P. Garcia-Del-Pino, "Time and orbital diversity assessment with Ka- and Q-band slant-path propagation experiments in Madrid," *IEEE Trans. Antennas Propag.*, vol. 67, no. 2, pp. 1193–1201, Feb. 2019, doi: 10.1109/TAP.2018.2882627.
- [12] E. Matricciani, "Time diversity in satellite links affected by rain: Prediction of the gain at different localities," in *Proc. 2nd Eur. Conf. Antennas Propag. (EuCAP)*, Nov. 2007, pp. 1–5, doi: 10.1049/ic.2007.1430.
- [13] N. W. M. Saad, A. F. Ismail, K. Badron, N. H. M. Sobli, J. Din, and T. A. Rahman, "Assessments of time diversity rain fade mitigation technique for V-band space-Earth link operating in tropical climate," *Int. J. Electr. Energy*, vol. 1, no. 4, pp. 268–273, 2013, doi: 10.12720/ijoe.1.4.268-273.
- [14] H. Fukuchi and T. Saito, "Novel mitigation technologies for rain attenuation in broadband satellite communication system using from Ka-to W-band," in *Proc. 6th Int. Conf. Inf., Commun., Signal Process.*, Dec. 2007, pp. 8–12.
- [15] Y.-Y. Ng, M. S. J. Singh, and V. Thiruchelvam, "Performance analysis of 60-min to 1-min integration time rain rate conversion models in Malaysia," *J. Atmos. Sol.-Terr. Phys.*, vol. 167, pp. 13–22, Jan. 2018, doi: 10.1016/j.jastp.2017.10.004.
- [16] P. Garcia-del-Pino, A. Benarroch, and J. M. Riera, "Comparison of recent rainfall rate models using Spanish data," in *Proc. 8th Eur. Conf. Antennas Propag. (EuCAP)*, Apr. 2014, pp. 42–45.
- [17] M. M. Alam, I. M. Rafiqul, K. Badron, D. A. R. Farah, A. K. Lwas, and H. Dao, "Time diversity gain analysis for Earth to satellite link based on measured rain rate," in *Proc. 7th Int. Conf. Comput. Commun. Eng. (ICCCCE)*, Sep. 2018, pp. 109–113.
- [18] E. Matricciani, "Probability distributions of rain attenuation obtainable with linear combining techniques in space-to-Earth links using time diversity," *Int. J. Satell. Commun. Netw.*, vol. 36, no. 2, pp. 220–237, Mar./Apr. 2018, doi: 10.1002/sat.1214.
- [19] E. Matricciani, "Time diversity as a rain attenuation countermeasure in satellite links in the 10–100 GHz frequency bands," in *Proc. 1st Eur. Conf. Antennas Propag. (ESASP)*, Nov. 2006, pp. 1–6.
- [20] D. B. Hodge, "An improved model for diversity gain on Earth-space propagation paths," *Radio Sci.*, vol. 17, no. 6, pp. 1393–1399, Nov./Dec. 1982, doi: 10.1029/RS017i006p01393.
- [21] *Propagation Data and Prediction Methods Required for the Design of Earth-Space Telecommunication Systems*, document ITU-R 618-12, 2015.
- [22] *Rain Height Model for Prediction Methods*, document ITU-R P.839-4, 2013.
- [23] *Characteristics of Precipitation for Propagation Modelling*, document ITU-R 837-7, 2017, vol. 6.
- [24] *Specific Attenuation Model for Rain for Use in Prediction Methods*, document ITU-R 838-3, 2005, pp. 1–5.
- [25] *Acquisition, Presentation and Analysis of Data in Studies of Tropospheric Propagation*, document ITU-R 311-18, 2021, pp. 311–318.
- [26] E. Matricciani, "Global formulation of the synthetic storm technique to calculate rain attenuation only from rain rate probability distributions," in *Proc. IEEE Antennas Propag. Soc. Int. Symp.*, Jul. 2008, pp. 1–4, doi: 10.1109/APS.2008.4619006.
- [27] M. M. Alam, I. M. Rafiqul, K. Badron, F. Dyana A. R., H. Dao, M. R. Hassan, and A. K. Lwas, "Investigation of time diversity gain for Earth to satellite link using rain rate gain," *Bull. Electr. Eng. Informat.*, vol. 8, no. 3, pp. 951–959, Sep. 2019, doi: 10.11591/eei.v8i3.1512.
- [28] A. K. Lwas, M. R. Islam, M. H. Habaebi, S. J. Mandeep, A. F. Ismail, and A. Zyoud, "Effects of wind velocity on slant path rain-attenuation for satellite application in Malaysia," *Acta Astronaut.*, vol. 117, pp. 402–407, Dec. 2015, doi: 10.1016/j.actaastro.2015.09.008.

- [29] M. M. Alam, M. R. Hasan, M. R. Islam, M. H. Habaebi, A. Basahel, and M. Singh, "Prediction of time diversity gain-comparison between ITU-R P. 618–13 using a concept of rain rate with delay and synthetic storm technique," *Int. J. Interact. Mobile Technol.*, vol. 16, no. 11, pp. 178–192, 2022.
- [30] A. F. Ismail and P. A. Watson, "Characteristics of fading and fade countermeasures on a satellite-Earth link operating in an equatorial climate, with reference to broadcast applications," *IEEE Proc. Microw., Antennas Propag.*, vol. 147, no. 5, pp. 369–373, Nov. 2000, doi: [10.1049/ip-map:20000704](https://doi.org/10.1049/ip-map:20000704).
- [31] M. M. Alam, M. R. Islam, M. A. Salam, and N. Muhammad, "Prediction of rain rate distribution with time delay based on measured 1-min rain intensity data to mitigate fades on satellite link," in *Proc. 7th Brunei Int. Conf. Eng. Technol. (BICET)*, Nov. 2018, pp. 1–4.
- [32] I. M. Rafiqul, A. K. Lwas, M. H. Habaebi, M. M. Alam, J. Chebil, J. S. Mandeep, and A. Zyoud, "Analysis of time diversity gain for satellite communication link based on Ku-band rain attenuation data measured in Malaysia," *Int. J. Elect. Comput. Eng.*, vol. 8, no. 4, pp. 2608–2613, 2018, doi: [10.11591/ijece.v8i4.pp2608-2613](https://doi.org/10.11591/ijece.v8i4.pp2608-2613).



MD. MOKTARUL ALAM (Member, IEEE) received the B.Sc. degree in electrical and electronic engineering from IBAIS University, Bangladesh, and the master's degree in electronic engineering from International Islamic University Malaysia. He is currently pursuing the D.Phil. degree with INSA Rennes. He is a Research Assistant with the Faculty of Electrical Engineering, ESEO, Angers, France. He is involved in electromagnetic compatibility research projects. He has published several research papers in national/international journals and conferences. His research interests include propagation, electromagnetic, and antennas.



MD. RAFIQU L ISLAM (Senior Member, IEEE) received the B.Sc. degree in electrical and electronic engineering from the Bangladesh University of Engineering and Technology, Dhaka, and the master's degree in electrical engineering, the Ph.D. degree in electrical engineering, and the Ph.D. degree from Universiti Teknologi Malaysia. He is currently a Professor with the Faculty of Electrical Engineering, International Islamic University Malaysia. He was a leader of several research projects and he also involved in various research projects in wireless communications. He also has a good teaching experience in the area of mobile radio communications, wireless communication systems, and antennas. He has published several review and research papers in national/international journals and conferences. His research interests include radio link design, RF propagation measurement and RF design, smart antennas, and array antennas design.



MOHSEN KOOHESTANI (Senior Member, IEEE) received the joint Ph.D. degree (Hons.) in electromagnetics from École Polytechnique Fédérale de Lausanne (EPFL), Lausanne, Switzerland, and Universidade de Lisboa (ULISBOA), Lisbon, Portugal, in 2014. From 2014 to 2018, he was a Senior Research Fellow with Institut d'Electronique et de Télécommunications de Rennes (IETR), University of Rennes 1, where he was working on the biomedical applications of wireless power transfer systems. He has been an Associate Professor with the ESEO School of Engineering, Angers, France, since 2018. He is currently an Associate Researcher with UMR CNRS 6164, Institute of Electronics and Telecommunications of Rennes (IETR). He has authored more than 70 peer-reviewed scientific articles. His research interests include the domain of antennas, microwaves, EMC, and biomedical engineering. He is an official member of the IEC Standardization Working Group (WG2 and WG9), SC47A French Subcommittee on the EMC for Integrated Circuits.



ELFATIH A. A. ELSHEIKH (Member, IEEE) received the B.Sc. degree in electrical and computer engineering from Omdurman Islamic University (OIU), Sudan, in 2000, the M.B.A. degree from the University of Khartoum (UoK), Sudan, in 2006, and the M.Sc. and Ph.D. degrees in electrical engineering from International Islamic University Malaysia (IIUM), in 2010 and 2017, respectively. He is currently an Assistant Professor with the Department of Electrical Engineering, College of Engineering, King Khalid University (KKU), Saudi Arabia. He has published more than 15 research papers in international journals and conferences. His research interests include wireless channel modeling, radio link design, RF propagation measurement, and modeling.

...